Association of a Platinum Complex to a G-Quadruplex Ligand Enhances Telomere Disruption

Razan Charif, Christine Granotier-Beckers, Hélène Charlotte Bertrand, Joel Poupon, Evelyne Seǵal-Bendirdjian, Marie-Paule Teulade-Fichou, Francois D Boussin, Sophie Bombard

Association of a Platinum Complex to a G-Quadruplex Ligand Enhances Telomere Disruption

Razan Charif,[†] Christine Granotier-Beckers,[‡] Hélène Charlotte Bertrand,[§,∥,⊥] Joël Poupon,[#] Evelyne Ségal-Bendirdjian,[†] Marie-Paule Teulade-Fichou,[§] François D. Boussin,[‡] and Sophie Bombard*[,†,§]

[†]Université Paris Descartes, INSERM UMR-S-1007, 45 rue des Saints-Pères, 75006 Paris, France

[‡]CEA/DRF/IRCM, Laboratoire de RadioPathologie, INSERM U967, Université Paris VII, Université Paris XI, 18 route du Panorama, 92265 Fontenay-aux-Roses Cedex, France

[§]Institut Curie, Centre Universitaire Paris Saclay, CNRS UMR9187/INSERM U1196, Bâtiments 110-112, 91405 Orsay, France

[∥]Département de Chimie, Ecole Normale Supérieure, PSL Research University, UPMC Univ Paris 06, CNRS, Laboratoire des Biomolécules (LBM), 24 rue Lhomond, 75005 Paris, France

[⊥]Sorbonne Universités, UPMC Univ Paris 06, Ecole Normale Supérieure, CNRS, Laboratoire des Biomolécules (LBM), 24 rue Lhomond, 75005 Paris, France

[#]Laboratoire de Toxicologie-Biologique, Hôpital Lariboisière, 2 rue Ambroise Paré, 75475 Paris, France

ABSTRACT: Telomeres protect the ends of chromosomes against illegitimate recombination and repair. They can be targets for G-quadruplex ligands and platinum complexes due to their repeated G-rich sequences. Protection of telomeres is ensured by a complex of six proteins, including TRF2, which inhibits the DNA damage response pathway. We analyzed telomere modifications induced in cancer cells by the experimental hybrid platinum complex, Pt-MPQ, comprising both an ethylene diamine monofunctional platinum complex and a G-quadruplex recognition moiety (MPQ). Pt-MPQ promotes the displacement of two telomeric proteins (TRF2 and TRF1) from telomeres, as well as the formation of telomere damage and telomere sister losses, whereas the control compound MPQ does not. This suggests that the platinum moiety potentiates the targeting of the G-quadruplex ligand to telomeres, opening a new perspective for telomere biology and anticancer therapy. Interestingly, the chemotherapy drug cisplatin, which has no specific affinity for G-quadruplex structures, partially induces the TRF2 delocalization from telomeres but produces less telomeric DNA damage, suggesting that this TRF2 displacement could be independent of G-quadruplex recognition.

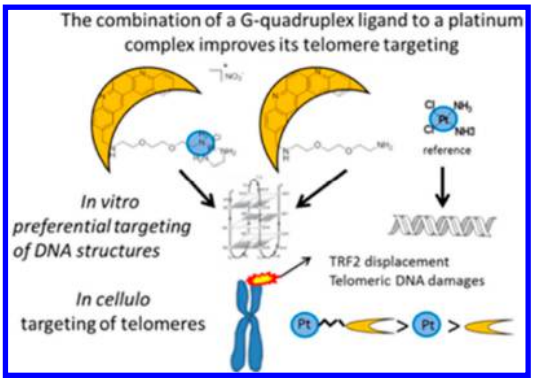

INTRODUCTION

Telomeres are specialized nucleoprotein complexes that are located at the end of chromosomes and protect them from degradation and illicit DNA repair activities.[1,2] Mammalian telomeres comprise tandemly repeated TTAGGG sequences, which protrude at the 3′-extremity by the G-rich single strand,[3] and shelterin, a complex of six specific proteins.[4] Among them are TRF1 and TRF2 (telomeric repeat binding factors 1 and 2), which bind, as homodimers, to the duplex part of telomeres via their myb-like domain,[5−7] and POT1, which binds to the single stranded TTAGGG DNA repeat.[8] These proteins recruit the other components, TIN2, RAP1, and TPP1. TRF1 and TRF2 are sufficiently abundant to cover the whole telomere with thousands of dimers.[9] Shelterin represses the activation of the ATM and ATR DNA damage responses. In particular, TRF2 inhibits ATM by a direct interaction with the region containing serine 1981 (S^{1981}), preventing the autophosphorylation of this residue necessary for the activation of this kinase.[10] Therefore, depletion of TRF2 activates the ATM kinase pathway, resulting in p53-mediated cell cycle arrest and DNA damage signal at telomeres. Besides, either deletion of TRF2 from mouse cells[10,11] or its inhibition with a dominant negative allele, $TRF2^{\Delta B\Delta M}$, in human cells[12−16] results in the accumulation of DNA damage factors such as 53BP1 and γ-H2AX at chromosome ends, as well as in telomere dysfunction-induced foci (TIFs) and in telomere processing by DNA repair pathways. Especially, chromosome end-to-end fusions are generated by the canonical nonhomologous end-joining (c-NHEJ) pathway.[17,18] The molecular mechanism by which

TRF2 prevents the NHEJ from acting on telomeres has not been completely resolved. TRF2 may impede NHEJ by promoting the formation of the t-loop,[19−21] a lasso-like structure that consists of the invasion of the G-overhang into the duplex part of telomeres.[22,23] Finally, TRF2 has been proposed to be a target for anticancer therapy since it seems to be involved in the tumorigenesis state[1,24−27] and is overexpressed in some tumor cells.[28,29] Moreover, the detection of TRF2 binding in extra-telomeric regions of chromosomes[30,31] suggests that TRF2 has also other biological roles.[32−34]

As telomeric DNA consists of repeated G-rich sequences, it can adopt a four-stranded stable DNA structure named the G-quadruplex structure. This noncanonical structure can be stabilized by specific ligands.[35−37] It has been shown that some G-quadruplex ligands induce displacement of TRF2[38−40] and/or of POT1 from telomeres.[39,41−43] In this case, telomere end fusions[41,42] are often associated with a loss of the G-overhang without affecting total telomere length.[43] However, the mechanism of action by which telomeres are deprotected via G-quadruplex ligands has not been fully clarified until now.[44,45] The current hypothesis is that the stabilization of G-quadruplex structures would impede the invasion of the G-overhang into the duplex part of the telomere, which is necessary to allow for the formation of the t-loop.[46] Moreover, the stabilization would induce the blockade of replication forks[47,48] by inhibiting helicases devoted to the resolution of G-quadruplex structures[49−51] and/or telomere aberrations generated by HR (homologous recombination) and NHEJ.[52] We have shown that G-quadruplex structures are potential *in vitro* targets for platinum complexes.[5354−58] Moreover, at the cellular level, the combination the G-quadruplex ligand **PDC**, also named 306A, (pyridodicarboxamide) with a *N*-heterocyclic carbene-platinum complex, **NHC-Pt**, already identified for its antitumor properties, results in a hybrid platinum complex (**NHC-Pt-PDC**) which induces an increased loss of TRF2 from the telomeres as compared to its respective constitutive moieties alone, **NHC-Pt** or **PDC**.[58] The question we address now is whether another hybrid molecule (**Pt-MPQ**) combining the G-quadruplex ligand (**MPQ**) with an ethylene diamine monofunctional platinum complex, which lacks antitumor properties, could also increase telomere targeting: indeed, **Pt-MPQ** preferentially targets G-quadruplex structures *in vitro* by cross-linking them irreversibly.[55] Cisplatin was also used as a reference anticancer drug[59] since it has no preference for G-quadruplexes[60] and in addition is known to induce DNA damage everywhere in the genome. Beside their differential recognition in DNA structures, these platinum complexes bind to DNA by different ways: while the ethylene diamine platinum can only bind to one purine, cisplatin binds preferentially to two adjacent guanines by forming 1,2 intrastrand GG adducts.[61] Moreover, the effects of cisplatin on telomeres remain controversial. Besides, cisplatin has been shown to alter telomere length of cancer cell lines,[62−65] but this effect strongly depends on the culture conditions used.[66] *In vitro*, it has been shown that telomeric sequences are not preferred targets for cisplatin, the amount of 1,2 intrastrand GG adducts being strictly proportional to the amount of adjacent guanines.[66−68] We also showed that an 1,2 intrastrand GG adduct of cisplatin induces a 20-fold reduction of the capacity of TRF2 to bind to telomeric DNA, while TRF1 binding was very little affected.[69] Furthermore, a platinated telomeric DNA 800 bp fragment inhibited the TRF2-dependent invasion process of the G-overhang.[69] These results suggest that cisplatin may affect TRF2 binding to telomeres *in cellulo*. Herein, we report telomere modifications induced by **Pt-MPQ** and cisplatin in the fibrosarcoma cell line HT1080. In particular, we show that **Pt-MPQ** promotes TRF2 and TRF1 delocalization from telomeres and increases the amount of telomere damage, more than the control compound **MPQ**, thereby suggesting that the association of the G-quadruplex ligand **MPQ** with a Pt complex triggers its ability to target telomeres. Additionally, we show that cisplatin is also able to induce the delocalization of TRF2 from telomeres but to a lesser extent than **Pt-MPQ**, suggesting that this delocalization can also be mediated by a non-G-quadruplex ligand. Furthermore, our results demonstrate that partial TRF2 displacement from telomeres does not systematically induce telomere damage or telomere aberrations.

MATERIALS AND METHODS

Cell Culture. The human fibrosarcoma cell line HT1080 (ATCC, American Type Culture Collection) was grown in DMEM medium completed by 2 mM of glutamine, 0.1 mg/mL of streptomycin, 100 U of penicillin, and 10% of fetal bovine serum (Gibco). Cells were treated with various concentrations of cisplatin, Pt-MPQ, or MPQ at 37 °C under humidity and 5% CO_2 conditions for 48 or 96 h. Cellular growth was quantified using the particle counter Z2 Coulter (Beckman, Coulter).

Cell Fixation and DNA Staining. HT1080 cells were trypsinized and fixed in 70% ethanol in PBS for 30 min at −20 °C. Cells were then centrifuged, resuspended in 1 mL of PBS containing 100 μg/mL RNase A and 40 μg/mL propidium iodide (Sigma, France) and incubated for 30 min at room temperature.[70]

Flow Cytometry. Cell cycle analysis was performed with a Coulter EPICS XL flow cytometer (Beckman-Coulter, France). The cell cycle profile was determined from the DNA fluorescence data using the ModFit 3.3LT software (Verity Software House, Topsham, Maine, USA).

Platinum Complexes. Cisplatin was provided from Sigma. Pt-MPQ and MPQ were synthesized following the procedure already described.[55] Aqueous solutions of 1 mM cisplatin, 1 mM Pt-MPQ and 2 mM MPQ (monopara-quinacridine) were prepared and conserved at −20 °C. Diluted solutions of each molecule were freshly prepared.

ChIP Assay for the Detection of TRF2, TRF1, and H3 Binding. ChIP was carried out using a Chromatin IP (ChIP) assay kit according to the manufacturer's instructions (Upstate). Cells were collected after fixation of proteins with formaldehyde and lysed. The DNA of the nucleus was sonicated until fragments of 1 kbp were obtained. 30 μL was conserved in order to quantify the number of telomeric sequences before immunoprecipitation (INPUT). Immunoprecipitation was then performed with anti-TRF2 polyclonal antibody (IMG-148A, IMGENEX), anti-TRF1 polyclonal antibody (ab1423, Abcam), antihistone H3 antibody (anti-H3, Abcam), or anti-IgG rabbit antibody (sc-2027, Abcam). 150 ng of the immunoprecipitated DNA and from INPUT was blotted onto a Hybond-XL membrane (Ge HealthCare). The telomere sequences were detected using a 800 bp telomere repeat (TTAGGG) ^{32}P labeled probe obtained after digestion of the pUC Telo2 plasmid[71] by *Eco*RI and *Bam*HI and radiolabeled by random priming using dCTP [α^{32}P], TAGGGTTA/TAACCCTA (Eurogentec) as primers and Klenow polymerase (Fermentas). The Alu sequences were detected using a ^{32}P labeled Alu probe that was obtained after the digestion of the pTopo Alu-AII plasmid (obtained after amplification of human genomic DNA with tgaaaccccgtctctactaaaaa and gtctcgctctgtcgccca primers, then cloned in pGEM-T vector (Promega)) by *Eco*RI and radiolabeled by random priming using dCTP [α^{32}P], the hexanucleotide mix (Roche) as primers and Klenow polymerase (Fermentas). The membranes were first hybridized with the telomere probe, and the amount of radioactivity was quantified using Phosphorimager and ImageQuant software. The membranes were dehybridized in boiling water containing 1% SDS and were then hybridized with the Alu probe; the amount of radioactivity was quantified using Phosphorimager and ImageQuant

software. Fold enrichment of the immunoprecipitated fraction compared to INPUT DNA is calculated as the ratio between telomeric DNA signals after precipitation and telomeric DNA signals in the total INPUT DNA for the same amount of blotted DNA (150 ng). The values are normalized to the Alu signal in the immunoprecipitated and INPUT fractions for each condition using the (telomere IP/telomere INPUT)/(Alu IP/Alu INPUT) formula. The % of TRF2 bound to telomeres was given as a function of TRF2 bound in treated cells/TRF2 bound in untreated cells.

Cell Cycle Analysis. Cell cycle status of HT1080 cells was determined by measuring DNA content using propidium iodide staining followed by flow cytometry analysis. HT1080 cells were trypsinized, then collected and fixed with 70% ethanol. A staining solution containing 40 μg/mL propidium iodide and RNaseA was added to cells for a 30 min incubation at 37 °C. Incorporated propidium iodide fluorescence intensity was quantified by flow cytometry at 488 nM laser excitation.

Western Blot. Western blots were performed following the Bio-Rad protocol. Briefly, 20 μg of proteins were electrophoresed in SDS–PAGE (SDS–polyacrylamide 10%) under denaturing conditions, then transferred to a PVDF membrane (polyvinylidin difluoride) (Amersham Hybond P $^{+}$, GE Healthcare), which was hybridized with mouse monoclonal anti-TRF2 antibody (4A794, Upstate) and antiactin HRP (SC1616-HRP, Santa-Cruz). TRF2 was revealed by the secondary antibody goat antimouse IgG-HRP (ab6789, abcam) using the ECL Western blotting detection reagent. Western-blot membranes were analyzed using the FluorChem software program.

Immunofluorescence. For interphase TRF2 foci analysis, HT1080 were plated on glass coverslips, fixed with 4% paraformaldehyde, and permeabilized in phosphate buffered saline (PBS) containing 0.5% Triton X-100, 3 mM $MgCl_2$, and 300 mM sucrose for 10 min at RT. Then, cells were incubated with the mouse monoclonal anti-TRF2 antibody (4A794, Upstate) for 2 h at RT, washed in PBS, and incubated with a goat antimouse IgG secondary antibody TRITC (tetramethylrhodamine)-conjugated (Thermofischer). Nuclei were counterstained with 4′,6-diamidino-2-phenylindole, Vectashield (DAPI). Three-dimensional images (composed of 40 to 80 planes of 0.3 μm) were acquired using an inverted microscope with an Epi-fluorescence attachment (Nikon Eclipse TE-2000 E). The number of TRF2 foci in each nucleus was counted using the ImageJ software program after a two-dimensional projection of three-dimensional images.

Telomere Dysfunction-Induced Foci (TIF) Analysis. Telo-FISH (telomere-fluorescence *in situ* hybridization) using peptide nucleic acid probes (PNA) conjugated to fluorescein isothiocyanate $(CCCTAA)_3$-FITC (PANAGENE) was combined with immunofluorescence (IF) using a monoclonal mouse anti γ-H2AX antibody (JBW301, Upstate) in order to detect interphase telomere dysfunction-induced foci (TIF). HT1080 plated on Chambered Coverglass (Lab-TeK, Nunc) were fixed with 4% paraformaldehyde, then they were washed in PBS and dehydrated using ethanol at progressive concentrations (70%, 80%, 90%, and 100%). 5 μg/mL of the PNA probe in hybridization mixture containing 70% formamide, 10 mM Tris-HCl at pH 7.2, 1 mM $MgCl_2$, and 0.5% Boehringer blocking reagent were added to cells, followed by DNA denaturation for 2 min at 75 °C and hybridization for 1 h and 30 min at room temperature. FISH protocol was followed by immunofluorescence staining, as previously described. Three-dimensional images (composed of 25 planes of 0.8 μm) were acquired using an inverted confocal microscope (Axiovert 200 M Zeiss LSM 510) in the SCM (Faculté des Sciences Fondamentales et Biomédicales, Université Paris Descartes). PNA foci, γ-H2AX foci, and TIF, where PNA foci and γ-H2AX foci colocalized, were counted in each nucleus from a two-dimensional projection of the three-dimensional images using the JACoP plugin of the ImageJ software program (NCBI).

Determination of Telomere Length. Genomic DNA was isolated from cells using a DNAeasy blood and tissue kit (Qiagen). An aliquot of 3 μg of DNA was digested overnight at 37 °C with restriction enzymes RsaI and HinfI. DNA fragments were separated by agarose gel electrophoresis and then transferred under denaturing conditions to a nylon membrane by Southern blotting. Telomere length was then estimated using the "Telo TAGGG Telomere Length Assay" kit (Roche).

Telo-FISH. HT1080 were cultured in their medium supplemented with cisplatin (1 and 5 μM), Pt-MPQ (5 μM), or MPQ (5 μM) at 37 °C for 96 h in a humidified atmosphere containing 5% CO_2. Cells were then incubated with colcemid (0.1 μg/mL, Sigma) at 37 °C for 2 h. After trypsinization and centrifugation (1500 rpm for 10 min), they were subjected to hypotonic swelling at 37 °C for 20 min. Metaphase preparations were then fixed in ethanol/acetic acid (3:1 v/v) overnight at 4 °C. The suspension was applied on cold wet slides, and the slides were air-dried overnight. Telo-FISH was carried out using a telomeric cyanine-3-conjugated $(C_3TA_2)_3$ PNA probe (Applied Biosystems) complementary to the G-rich telomeric strand, as described in detail by Pennarun et al.[79] Metaphases were counterstained with DAPI (1 μg/mL), mounted in Fluoromount-G (Southern Biotech) and observed under a fluorescence microscope (Olympus AX70).

Platinum Quantification. The platinum cellular uptake was quantified by ICP-MS (inductively coupled plasma mass spectrometry) on the cellular pellet or DNA extract of HT1080 cells treated during 96 h with cisplatin or Pt-MPQ.

TUNEL Assay. HT1080 cells were treated with the different drugs at doses inducing 85% growth inhibition during 96 h or 10 μM cisplatin for 24 h, fixed in paraformaldehyde, permeabilized with 70% ethanol. Apoptotic cells were quantified by the TUNEL assay, using the In Situ Cell Death Detection Kit, TMR red (Roche) according to the manufacturer's instructions, before observation under a fluorescence microscope.

RESULTS

Antiproliferative Properties of Pt-MPQ Compared to Those of MPQ and Cisplatin. HT1080 cells were treated with increasing doses of Pt-MPQ, MPQ, and cisplatin (Figure 1) for 96 h. Dose–response curves evidenced that Pt-MPQ

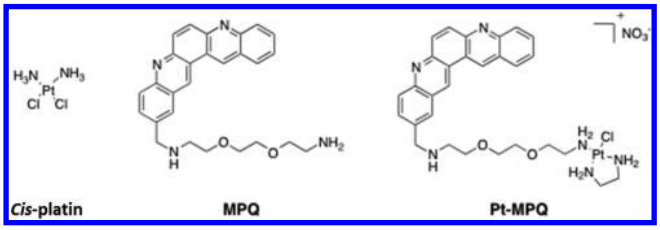

Figure 1. Chemical structure of cisplatin, MPQ, and Pt-MPQ.

induced 50, 70, and 80% cell growth inhibition at 2, 4, and 5 μM, respectively (Figure 2A), while only 30% growth inhibition was obtained with 5 μM of MPQ, indicating that addition of the platinum atom enhances the antiproliferative activity of MPQ, whereas, 0.8, 1, and 1.3 μM of cisplatin induced 50, 70, and 80% cell growth inhibition, respectively.

To gain further insight into differential proliferation growth inhibition of cisplatin and Pt-MPQ, we quantified the amount of platinum complex uptake and the amount of platinum bound to DNA after 96 h of treatment at doses inducing the same inhibition of cell proliferation: 5 μM Pt-MPQ and 1.3 μM cisplatin. The amount of Pt-MPQ uptake is about 20-fold higher than that observed for cisplatin (26 ng of Pt and 1.3 ng Pt/5 $\times$ 10^6 cells, respectively) as evaluated by ICP-MS Pt dosage. However, quite remarkably, the amount of platinum bound to DNA was almost the same (about 250 pg Pt/mg DNA). Therefore, the same amount of platinum bound to DNA required higher Pt-MPQ intracellular accumulation than cisplatin, as already described for many other platinum complexes.[58,72] Since the inhibition of cell proliferation of Pt-MPQ and cisplatin could be related to their level of DNA

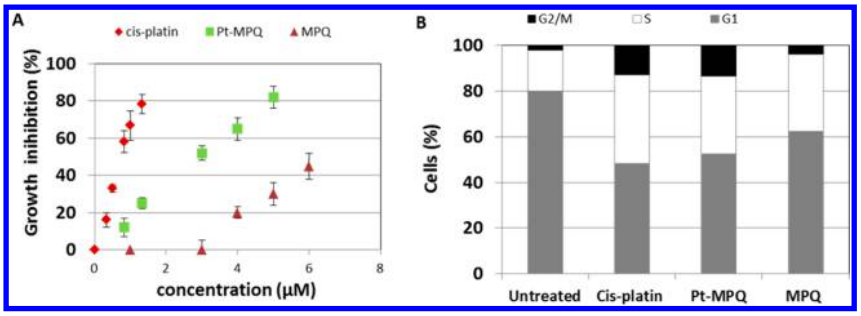

Figure 2. HT1080 inhibition, cell proliferation, and synchronous cell cycle progression. (A) % growth inhibition of HT1080 cells by cisplatin, Pt-MPQ, and MPQ. (B) HT1080 cells were treated with doses of cisplatin and Pt-MPQ that induce 80% cell growth inhibition (1.3 and 5 μM, respectively) for 96 h. MPQ that serves as the control for Pt-MPQ was used at 5 μM. Cells were collected and processed by FACS analysis of DNA content. The histogram shows the distribution of cells in the different phases of the cell cycle based on the DNA fluorescence intensity of propidium iodide (DNA content).

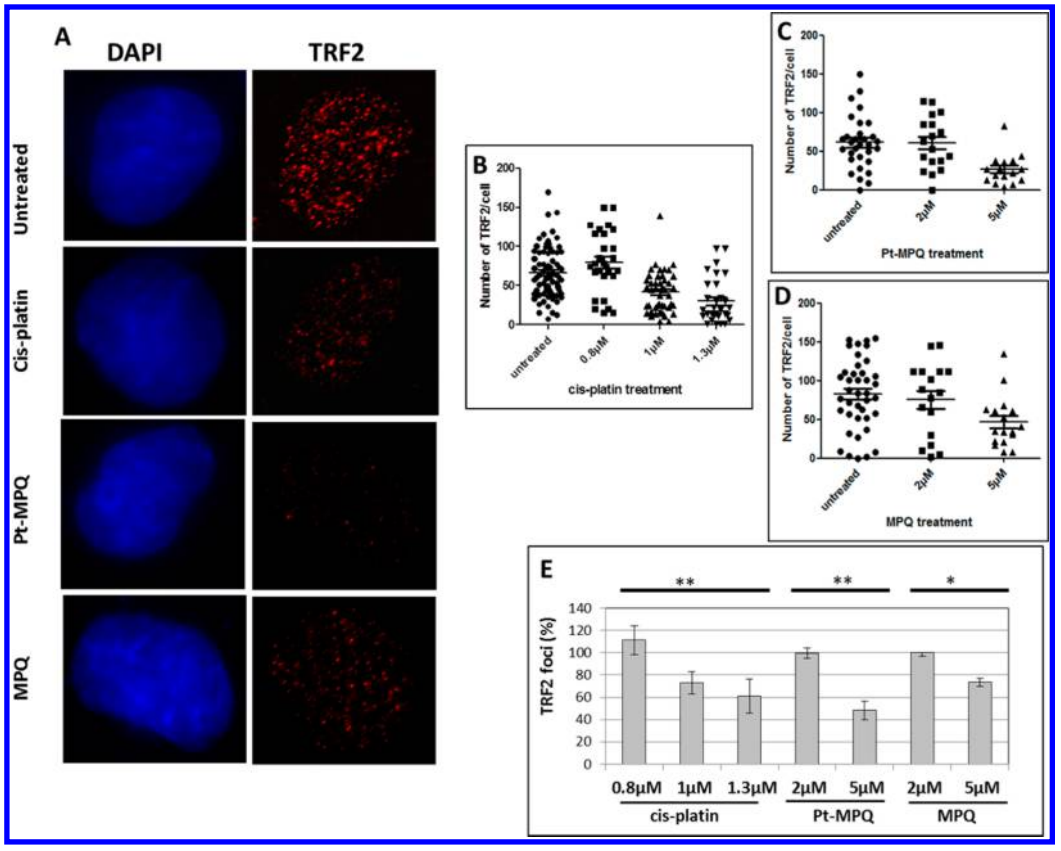

Figure 3. TRF2 foci quantification detected by immunofluorescence on HT1080 treated with cisplatin, Pt-MPQ, and MPQ for 96 h. Cells were processed for immunofluorescence using antibodies against TRF2 (A). The number of TRF2 foci for a typical experiment after (B) cisplatin, (C) Pt-MPQ, and (D) MPQ treatments showing the diversity of cells. (E) % of TRF2 foci after HT1080 cell treatments with cisplatin, Pt-MPQ, and MPQ (mean of at least 3 experiments). ** Indicates a Mann and Withney test *P*-value <0.01 and *$P < 0.05$ (GraphPad PRISM software).

binding,[73,74] we analyzed the cellular effect of each compound at doses that induce both the same amount of platinum bound to DNA and the same percentage of growth inhibition, i.e., the same drug potency. The cell cycle progression of treated cells shows enrichment for cells in S phase for all compounds and in G2/M for cisplatin[72] and for Pt-MPQ (Figure 2B and Figure S1A). In these conditions, only a low level of apoptosis was found for adherent cells, as shown by the small percentage of sub-G1cells (<5%) (Figure S1B) and te TUNEL assay (Figure S2). In addition, only a small fraction of apoptotic floating cells (<10%) was also observed (Figure S2). Therefore, only the telomeres of adherent treated cells that were still viable were analyzed.

TRF2 Displacement from Telomeres upon Treatment with Pt-MPQ, MPQ, and Cisplatin. TRF2 is a major component of shelterin, which binds to telomeres and ensures their integrity.[4] Since TRF2/DNA interaction can be strongly affected by G-quadruplex ligands, the amount of TRF2 foci and TRF2 bound to telomeres after the various treatments were quantified. Using immunostaining,[39,75,76] we showed that the number of TRF2 foci decreases as a function of concentration (Figure 3) and time (Figure S4) for all three compounds. However, Pt-MPQ is more prone to delocalize TRF2 than MPQ and cisplatin. Indeed, immunofluorescence revealed 45%, 60%, and about 80% of remaining TRF2 foci in cells treated for 96 h with Pt-MPQ, cisplatin, and MPQ, respectively.

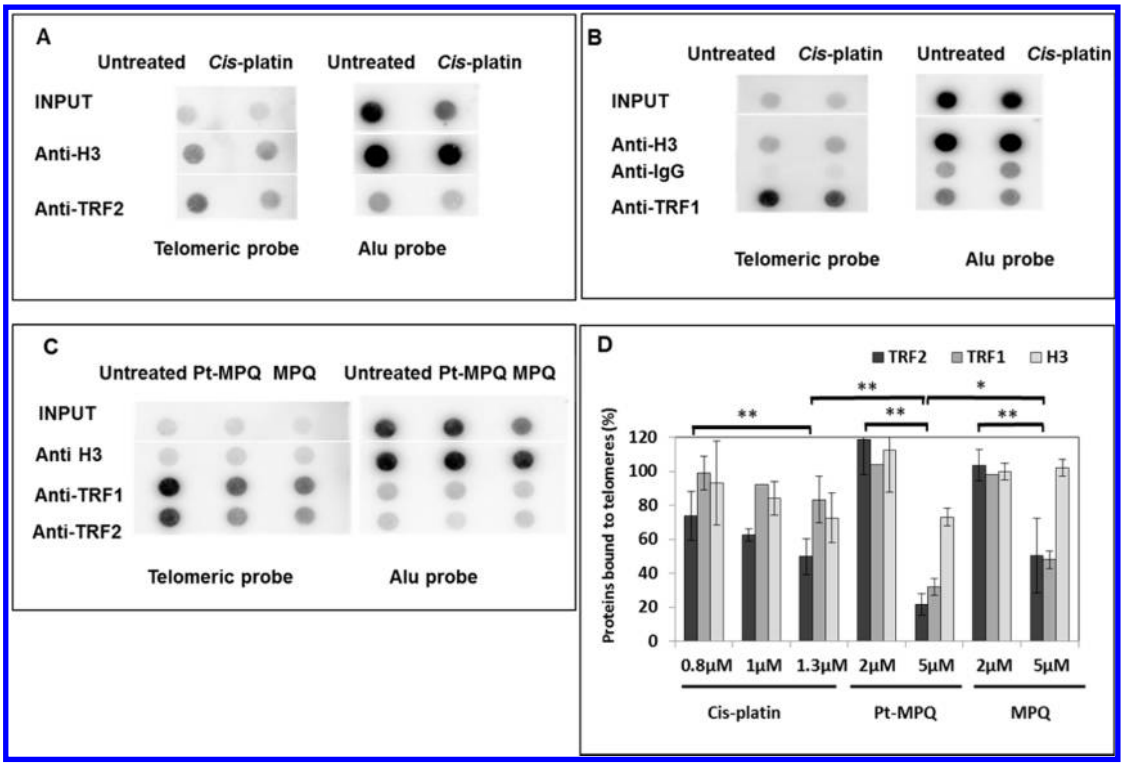

Figure 4. Proteins bound to telomeres quantified from dot-blots. ChIP on HT1080 cells treated with doses of cisplatin (A and B), Pt-MPQ, and MPQ (C) that induce the maximum cell growth inhibition (1.3, 5, and 5 μM, respectively) for 96 h with anti-H3, anti-TRF1, and anti-TRF2 antibodies. % of proteins bound to telomeres (D). Telomeric sequences were evidenced in a DNA fraction immunoprecipitated by an anti-TRF1, anti-TRF2 (or anti-H3) antibody using a ^{32}P radiolabeled 800 pb telomeric probe and normalized with α ^{32}P radiolabeled Alu sequences in untreated, cisplatin, Pt-MPQ, and MPQ treated cells. An anti-IgG antibody was used as a negative control. An anti-H3 antibody was used as the positive control. 200 ng of DNA was blotted for each sample. The % represents the quantitative values of telomeric DNA signals in the samples originating from cells with treatment compared to the cells without any treatment. Quantitative values of telomeric DNA signals are calculated as the ratio between telomeric DNA signal precipitation and telomeric DNA signals in the INPUT for the same amount of blotted DNA. These values have been normalized by the amount of blotted DNA for each sample quantified by the nonspecific Alu probe, following the formula (telomere IP/telomere INPUT)/(Alu IP/Alu INPUT) (means of at least 3 experiments). ** Indicates a Mann and Withney test *P*-value <0.01 and * $P < 0.05$ (GraphPad PRISM software). Statistical analysis was made by comparing the amount of TRF2 bound to telomeres for each treatment at different doses and between each treatment at the highest dose. Blots have been cropped in order to improve the clarity and conciseness of the presentation. Full-length blots are presented in Figure S6.

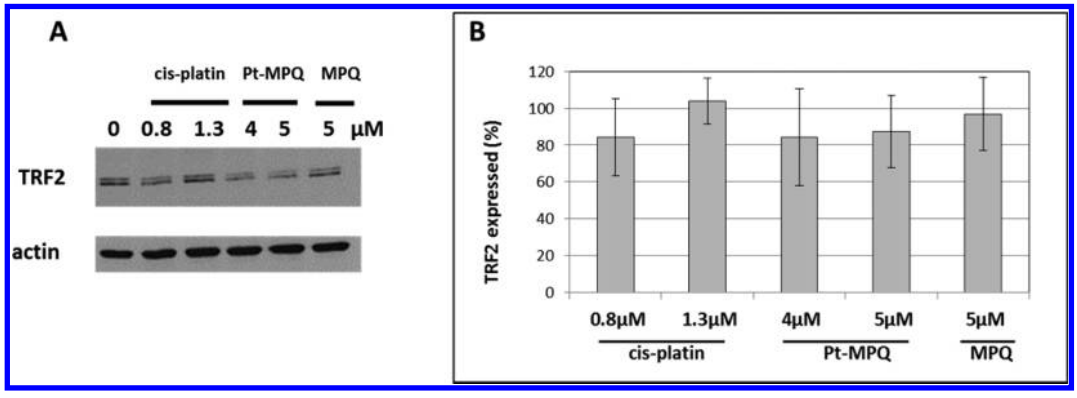

Figure 5. Western blot of TRF2 from HT1080 cells treated by cisplatin, Pt-MPQ, and MPQ for 96 h. (A) Membranes and (B) percentage of TRF2 expression normalized with actin (mean of 3 experiments).

The amounts of TRF2, TRF1, and histone H3 bound to telomeres in treated cells were also performed by ChIP experiments (Figure 4 and Figure S5). ChIP results confirmed the ones obtained from immunostaining for TRF2. They evidenced that Pt-MPQ induces a dose-dependent decrease of TRF2 and TRF1 at telomeres, respectively, reaching 80 and 75% of protein loss. MPQ is less efficient (50% decrease of both TRF1 and TRF2). It is noteworthy that cisplatin delocalizes 50% of TRF2 protein and slightly affects TRF1 binding (15% delocalization). In contrast to TRF1 and TRF2 binding, H3 binding to telomeres was only slightly affected by Pt-MPQ treatment.

Since the decrease of TRF2 bound to telomeres could result from a decrease in TRF2 expression (due to the stabilization of

the G-quadruplex structures within its 5′UTR mRNA region[77]), TRF2 expression was analyzed by Western blot. TRF2 appeared as a double band, as previously described.[9] TRF2 expression was not significantly affected by Pt-MPQ, MPQ, or cisplatin treatments, excluding a reduced amount of cellular TRF2 (Figure 5). Therefore, our results show that Pt-MPQ, MPQ, and cisplatin are able to delocalize TRF2 from telomeres.

TRF2 Displacement from Telomeres upon Treatment with Pt-MPQ, MPQ, and Cisplatin Did Not Induce Telomere Length Shortening. Even though a short erosion of telomeres could not be excluded, Southern blot analysis of the mean value of TRF (telomere restriction fragments) showed that the different treatments did not induce any telomere length shortening (Figure 6).

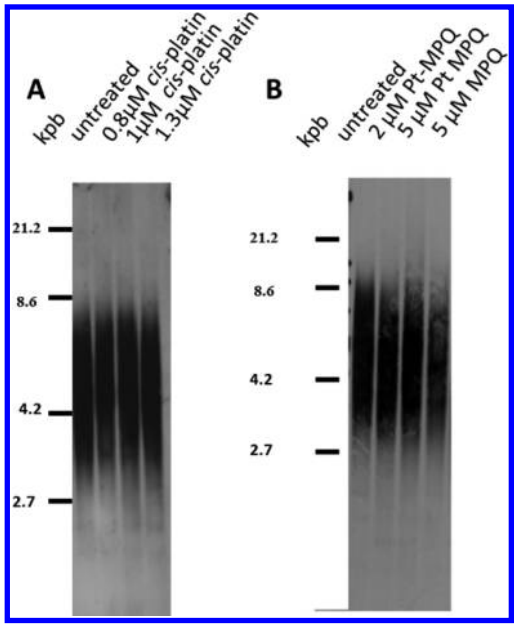

Figure 6. Telomere length from HT1080 untreated and treated cells with (A) cisplatin, (B) Pt-MPQ, and MPQ for 96 h with indicated doses.

Pt-MPQ Increases the Amount of Damage to Telomeres and a Partial Loss of Telomeres. As loss of TRF2 from telomeres can also induce a telomeric DNA damage response, as evidenced by the detection of telomere dysfunction-induced foci (TIFs),[14] we first investigated genomic DNA damage signaling in treated cells by γ-H2AX immunostaining (γ-H2AX foci), a marker for DNA damage induced by platinum complexes.[78] As expected, cisplatin induced a large amount of genomic DNA damage (Figure 7A and B). Similarly, a large number of γ-H2AX foci were detected upon Pt-MPQ treatment, whereas MPQ alone did not induce any γ-H2AX foci (amount similar to that depicted in untreated cells) (Figure 7A and B). These data suggest that the presence of a platinum atom is crucial to trigger DNA damage. Telomere damage response was assessed by the quantification of γ-H2AX foci at telomeres using a telomeric PNA probe. A 20% decrease in the number of PNA foci after 96 h of treatment by Pt-MPQ has been observed (Figure S4). This result suggests that Pt-MPQ could prevent the binding of the PNA probe. Therefore, shorter treatments have been envisioned, and the 48 h-treatment has been chosen. In this condition, the treatments still induce 45−55% TRF2 delocalization (Figure S3) without reducing the number of PNA foci (Figure 7C). Co-localization of the DNA damage signals with telomeres showed that 47% (average 1.8 TIFs per cell) and 15% (0.7 TIFs per cell) of cells treated with Pt-MPQ and cisplatin, respectively, contain telomeric DNA damage (2−7 per cells) (Figure 7D).

Pt-MPQ and Cisplatin Treatments Induce Telomere Aberrations. In order to gain further insight on telomere dysfunctions induced by the different compounds, we analyzed telomere aberrations in metaphase chromosomes of cells treated for 48 h (Figure 8 and Figure S6). Telo-FISH confirmed that both cisplatin and Pt-MPQ induced much more numerous telomere aberrations than MPQ. They both induced a very high number of sister telomere losses and to a lesser extent sister telomere fusions and terminal deletions but had no effect on telomere doublets. Sister telomere losses are the consequence of damage that occurred during or after telomere replication.[79,80] Both compounds also induced radians and chromatid breaks resulting from nontelomeric DNA breaks also occurring after replication. Interestingly, cisplatin and Pt-MPQ considerably induced more sister telomere losses than radians and chromatid breaks, showing preferential targeting of telomeric sequences by the two compounds.

DISCUSSION

The aim of this work was based on three assumptions. First, we wanted to determine if the combination within the same molecule of the G-quadruplex ligand MPQ and a platinum complex (Pt-MPQ) could improve telomere targeting. Indeed, *in vitro*, Pt-MPQ binds covalently and exclusively to three guanines of the top G-quartet of telomeric G-quadruplex structure.[55] Moreover, its kinetic of platination is 6 times faster for the G-quadruplex than the duplex structure,[55] confirming the preference of Pt-MPQ for the G-quadruplex structure. Second, since controversial conclusions exist about the possible role of cisplatin on telomere length modification *in cellulo*,[66] we wanted to establish if cisplatin was able to modify telomere structure. Third, we wanted to determine to what extent both kinds of complexes were able to displace TRF2 from telomeres. TRF2 has a major role in protecting telomeres from illicit recombination since the removal of TRF2 from telomeres results in end-to-end fusions and rapid induction of cell cycle arrest.[10−16] Moreover, TRF2 is emerging as a potential target in cancer therapy[24] as it is highly expressed in some cancer cells.[24,28,81−84] Herein, we show that Pt-MPQ increases telomere targeting compared to MPQ by inducing TRF2 delocalization and telomeric DNA damages. Moreover, cisplatin is also able to induce the delocalization of TRF2 from telomeres, however to a lesser extent than Pt-MPQ, suggesting that the mechanism of TRF2 delocalization from telomeres can also be driven by a non-G-quadruplex ligand. Furthermore, using the differential telomeric response of Pt-MPQ, MPQ, and cisplatin, we clearly show that there is no correlation between TRF2 delocalization and telomere aberrations.

Pt-MPQ More Efficiently Targets Telomeres than MPQ. The amount of TRF2 and TRF1 bound to telomeric DNA was assessed both by ChIP and immunostaining experiments because these methods might under- or over-estimate the amount of proteins. In the ChIP assay, the amount of pulled-down telomeric DNA, which is about 1 kb, is not necessarily proportional to the amount of telomeric protein bound. In fact, many dimers of TRF1 and TRF2 could be bound to these fragments,[9] and consequently, the quantification might be underestimated and the real amount of remaining

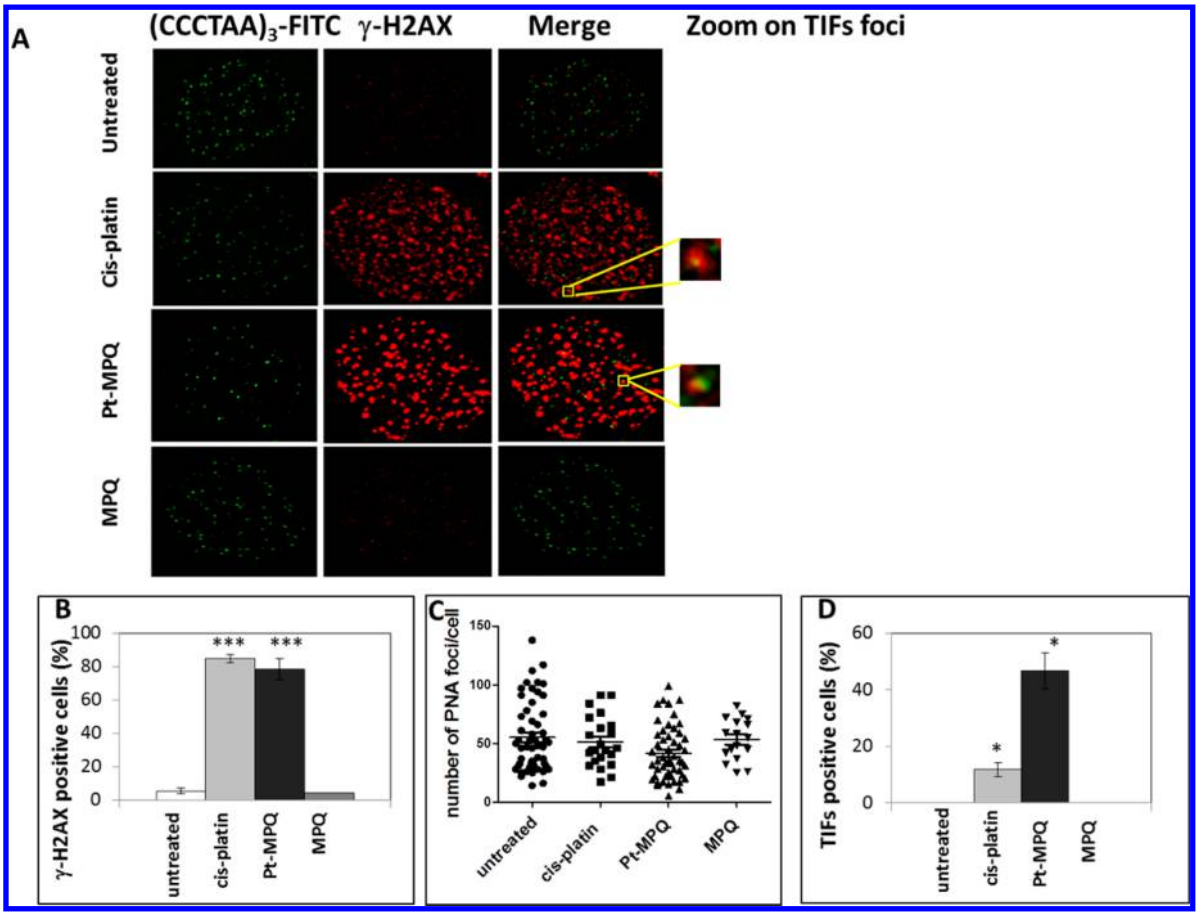

Figure 7. DNA damage activation at telomeres. HT1080 cells were treated for 48 h with cisplatin, Pt-MPQ, and PMQ at doses that induce 80% growth inhibition at 96 h. Cells were processed for immunofluorescence using antibodies against γ-H2AX and a C-rich PNA telomeric probe. (A) Z project of microscopy confocal acquisitions of cells treated with cisplatin and Pt-MPQ. (B) Percentages of γ-H2AX positive cells. (C) Number of PNA foci in untreated and treated cells with cisplatin and Pt-MPQ. (D) Percentages of TIFs positive cells in untreated and treated cells. Cells with more than 20 γ-H2AX foci and 2 TIFs were scored as γ-H2AX and TIF positive, respectively (mean of at least 3 experiments). *** Indicates a Mann and Withney test *P*-value <0.001 and * $P < 0.05$ (GraphPad PRISM software).

proteins minimized. Immunofluorescence experiments allow the visualization of TRF2 foci at the level of the individual cell. However, since TRF2 binds to extra-telomeric sequences,[30,31] the amount of foci was not necessarily representative of the total amount of TRF2 bound to telomeres. Hence, both methods are complementary. By comparing the relative TRF2 displacement as a function of treatments, the results obtained from ChIP are in agreement with those from immunofluorescence. However, from a quantitative point of view, a variation between both methods has been observed and reflects the fact that immunofluorescence and ChIP experiments could over- and underestimate, respectively, the amount of TRF2 bound to telomeres.

Previous studies show that the combination, within the same molecule of a platinum moiety with PDC, a G-quadruplex ligand (also called pyridodicarboxamide bisquinolinium derivative or 360A) that was already shown to preferentially localize at telomeres,[85] increases TRF2 delocalization from telomeres compared to the ligand alone.[58] Here, we evidenced that (i) delocalization of telomeric proteins (TRF1 and TRF2) is greater in cells treated with Pt-MPQ than in those cultured with MPQ (Figure 3D), (ii) the percentage of cells with DNA damage foci induced by telomere dysfunction-induced foci (TIF) reached about 40% after Pt-MPQ treatment, while there were none detected with MPQ (Figure 7D), and (iii) Pt-MPQ triggers the formation of specific telomere aberrations (sister telomere losses and sister telomere fusions, Figure 8), while MPQ did not.

Altogether, these results clearly evidenced that Pt-MPQ (G-quadruplex ligand combined with a platinum complex) more efficiently targets telomeres than MPQ (G-quadruplex ligand without platinium complex).

We can speculate that this result can be associated with the covalent binding of the hydrid platinum complex to telomeric G-quadruplex structures which could impede more efficiently the unfolding of G-quadruplexes and prevent their unwinding by helicases.[86−89]

Although Pt-MPQ appears to be more specific at telomere targeting than cisplatin, it also induces genomic DNA damage (γ-H2AX foci). This indicates that the target of Pt-MPQ is not restricted to telomeres. As mapped by bioinformatics surveys[90] and revealed by antibodies[91,92] as well as recent high-throughput sequencing,[93] G-quadruplex structures could also be formed in other G-rich regions of the genome. Therefore, Pt-MPQ could target these G-rich regions and/or other nonspecific sequences.

Cisplatin Targets Telomeres Less Efficiently than Pt-MPQ. TRF2 binding to telomeres is also affected by cisplatin, suggesting the mechanisms leading to TRF2 displacement from telomeres does not necessarily depend on G-quadruplex

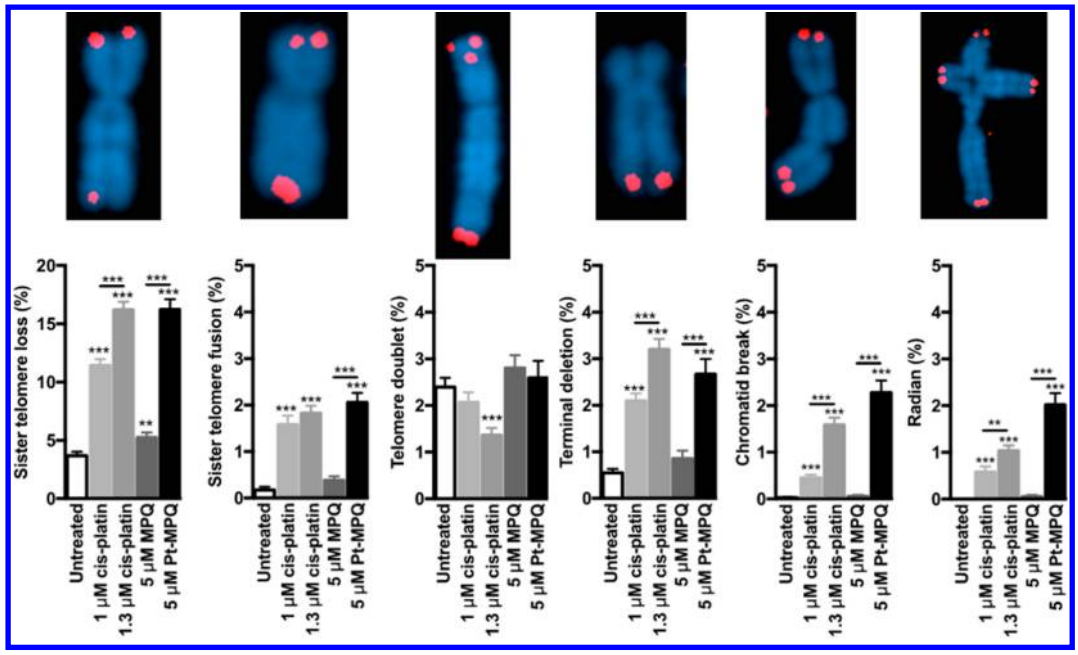

Figure 8. Cisplatin and Pt-MPQ induce mainly sister telomere losses in HT1080. Metaphases of HT1080 cells were collected after 48 h of treatment with 1 and 1.33 μM cisplatin, 5 μM Pt-MPQ, or 5 μM MPQ. Telomeres were hybridized with a telomere Cy3-PNA probe (red), and chromosomes were counterstained with DAPI (blue). Histograms show the percentages of metaphase chromosomes with the indicated telomere aberration detected by Telo-FISH (sister telomere loss, terminal deletion, sister telomere fusion, and telomere doublet) and the percentages of chromatid breaks and radians ± standard error of the mean (n = 5567−11473 chromosomes analyzed per condition). ** Indicates a t test P-value <0.01 and *** P < 0.0001 (GraphPad PRISM software).

targeting. The displacement of TRF2 from telomeres induced by cisplatin could be partly explained by our *in vitro* studies: TRF2 binding to platinated telomeric DNA is more affected than TRF1 binding,[69] suggesting that the steric hindrance of platinum chelates impedes more efficiently the binding of TRF2 than that of TRF1, which is more tightly bound to telomeres,[94] although this hypothesis still remains to be demonstrated.

Partial TRF2 Displacement from Telomeres Does Not Induce Telomere Shortening. Telomere length was not affected by the different treatments despite 50%−80% displacement of TRF2. This observation suggests that 20%−50% TRF2 bound to telomeres is still sufficient to preserve telomere length. These results are in agreement with other studies showing that a minimum amount of TRF2 bound to telomeres is sufficient to maintain telomere length. As has been reported using shRNA directed against TRF2, 10% of TRF2 bound to telomeres is thought to preserve telomere integrity,[9] and only a total removal of TRF2 and TRF1 induces telomere dysfunction.[95] All these data indicate that TRF2 displacement from telomeres does not systematically trigger telomere length shortening.

TRF2 Displacement from Telomeres Is Not Always Associated with Telomeric Instability. Our results further show that TRF2 displacement does not necessarily induce telomere dysfunctions and aberrations. In previous reports, telomere damage (TIFs) has been observed in cells expressing the dominant-negative TRF2$^{\Delta B\Delta M}$ allele, lacking TRF2 or treated by the G-quadruplex ligand.[11,14,76,96] In this study, only Pt-MPQ and cisplatin were able to induce telomere damage, whereas MPQ was not, despite the fact that they all delocalize TRF2 from telomeres. This result strongly supports the idea that TIFs formation is not systematically associated with TRF2 delocalization.

Telomere aberrations in metaphase spreads are another characteristic mark of telomere dysfunctions. Such aberrations have been detailed in cells expressing nonfunctional TRF2[12,13] or in cells treated with G-quadruplex ligands such as 360A[52,80] and RHPS4.[47] Both Pt-MPQ and cisplatin induce a major telomeric instability that occurred after replication (sister telomere losses) and, to a lesser extent, to sister telomere fusions. However, these telomere aberrations have not been depicted after MPQ treatment. This result reinforces the notion that there is no correlation between telomere aberrations and TRF2 displacement from telomeres.

In conclusion, we provide evidence that platinum derivatives are able to modify telomere structures independently to their capacity to stabilize G-quadruplex structures and we confirm that a platinum complex associated with a G-quadruplex ligand within the same molecular scaffold increases targeting of telomeres compared to that of the ligand alone.[58] This finding suggests that targeting telomeres by platinum complexes could be a new way to explore anticancer therapy. Our work also suggests no correlation between TRF2 delocalization and telomere dysfunctions: a partial displacement of TRF2 from telomeres is unable to induce telomere shortening and can occur without generating telomere aberrations.

■ ASSOCIATED CONTENT

HT1080 cell cycle progression in the presence of cisplatin or Pt-MPQ; TUNEL staining on adherent HT10 80 cells treated with cisplatin or Pt-MPQ; TRF2 foci quantification detected by immunofluorescence on HT1080 treated with cisplatin, Pt-MPQ, and MPQ for

24, 48, 72, and 96 h; number of PNA foci in untreated and treated cells with cisplatin and Pt-MPQ for 48 h and 96 h; full-length blots of Figure 4; and Telo-FISH on metaphase spreads from HT1080 control cells or treated for 48 h with MPQ, cisplatin, or Pt-MPQ (PDF)

AUTHOR INFORMATION

Corresponding Author

*Phone: 00 33 1 69 86 31 89. E-mail: sophie.bombard@curie.fr.

ORCID

Sophie Bombard: 0000-0002-6543-4497

Author Contributions

R.C. did the main experiments. C.G.B. did the telomere aberration experiments, wrote the manuscript, and prepared Figure 8. H.C. B. did the synthesis of Pt-MPQ. J.P. did the ICP-MS measurements. E.S.B. participated in the writing of the manuscript. M.P.T.F. participated in the synthesis of Pt-MPQ and wrote the manuscript. F.D.B. participated in the telomere aberration experiments and wrote the manuscript. S.B. participated in the experiments, wrote the manuscript text, and prepared the figures.

Funding

This work was supported by the Association pour la Recherche sur le Cancer (ARC grant 4835 to the S.B. team). We also thank the EU-COST action CM1105, INSERM (Institut National de la Santé et de la Recherche Médicale) and CNRS (Centre National de la Recherche Scientifique) for financial support.

Notes

The authors declare no competing financial interest.

ACKNOWLEDGMENTS

We thank Annie Munier for technical help with flow cytometry analysis. Flow cytometry was carried out at the Institute of Biology Paris-Seine Imaging Facility, which is strongly supported by the "Conseil Regional Ile-de France", the French national research councils (CNRS and INSERM), and Sorbonne University, UPMC Univ Paris 06. We sincerely acknowledge the SCM (Service Commun de Microscopie - *Faculté des Sciences Fondamentales et Biomédicales – Université Paris Descartes*).

ABBREVIATIONS

TRF1, telomeric repeat binding factor 1; TRF2, telomeric repeat binding factor 2; ATM, ataxia telangiectasia mutated; ATR, Ataxia telangiectasia; c-NHEJ, canonical nonhomologous end-joining; TRF, telomere restriction fragments; TIF, telomere dysfunction-induced foci

REFERENCES

(1) Blasco, M. A. (2005) Telomeres and human disease: ageing, cancer and beyond. *Nat. Rev. Genet.* *6*, 611−622.

(2) de Lange, T. (2005) Shelterin: the protein complex that shapes and safeguards human telomeres. *Genes Dev.* *19*, 2100−2110.

(3) de Lange, T. (2002) Protection of mammalian telomeres. *Oncogene* *21*, 532−540.

(4) Palm, W., and de Lange, T. (2008) How shelterin protects mammalian telomeres. *Annu. Rev. Genet.* *42*, 301−334.

(5) Bilaud, T., Koering, C. E., Binet Brasselet, E., Ancelin, K., Pollice, A., Gasser, S. M., and Gilson, E. (1996) The telobox, a Myb-related telomeric DNA binding motif found in proteins from yeast, plants and human. *Nucleic Acids Res.* *24*, 1294−1303.

(6) Broccoli, D., Smogorzewska, A., Chong, L., and de Lange, T. (1997) Human telomeres contain two distinct Myb-related proteins, TRF1 and TRF2. *Nat. Genet.* *17*, 231−235.

(7) Court, R., Chapman, L., Fairall, L., and Rhodes, D. (2005) How the human telomeric proteins TRF1 and TRF2 recognize telomeric DNA: a view from high-resolution crystal structures. *EMBO Rep.* *6*, 39−45.

(8) Baumann, P., and Cech, T. R. (2001) Pot1, the putative telomere end-binding protein in fission yeast and humans. *Science* *292*, 1171−1175.

(9) Takai, K. K., Hooper, S., Blackwood, S., Gandhi, R., and de Lange, T. (2010) In vivo stoichiometry of shelterin components. *J. Biol. Chem.* *285*, 1457−1467.

(10) Denchi, E. L., and de Lange, T. (2007) Protection of telomeres through independent control of ATM and ATR by TRF2 and POT1. *Nature* *448*, 1068−1071.

(11) Celli, G. B., and de Lange, T. (2005) DNA processing is not required for ATM-mediated telomere damage response after TRF2 deletion. *Nat. Cell Biol.* *7*, 712−718.

(12) Karlseder, J., Broccoli, D., Dai, Y., Hardy, S., and de Lange, T. (1999) p53- and ATM-dependent apoptosis induced by telomeres lacking TRF2. *Science* *283*, 1321−1325.

(13) Smogorzewska, A., and de Lange, T. (2002) Different telomere damage signaling pathways in human and mouse cells. *EMBO J.* *21*, 4338−4348.

(14) Takai, H., Smogorzewska, A., and de Lange, T. (2003) DNA damage foci at dysfunctional telomeres. *Curr. Biol.* *13*, 1549−1556.

(15) d'Adda di Fagagna, F., Reaper, P. M., Clay-Farrace, L., Fiegler, H., Carr, P., Von Zglinicki, T., Saretzki, G., Carter, N. P., and Jackson, S. P. (2003) A DNA damage checkpoint response in telomere-initiated senescence. *Nature* *426*, 194−198.

(16) Dimitrova, N., and de Lange, T. (2006) MDC1 accelerates nonhomologous end-joining of dysfunctional telomeres. *Genes Dev.* *20*, 3238−3243.

(17) van Steensel, B., Smogorzewska, A., and de Lange, T. (1998) TRF2 protects human telomeres from end-to-end fusions. *Cell* *92*, 401−413.

(18) Dimitrova, N., and de Lange, T. (2009) Cell cycle-dependent role of MRN at dysfunctional telomeres: ATM signaling-dependent induction of nonhomologous end joining (NHEJ) in G1 and resection-mediated inhibition of NHEJ in G2. *Mol. Cell. Biol.* *29*, 5552−5563.

(19) Griffith, J. D., Comeau, L., Rosenfield, S., Stansel, R. M., Bianchi, A., Moss, H., and de Lange, T. (1999) Mammalian telomeres end in a large duplex loop [see comments]. *Cell* *97*, 503−514.

(20) Stansel, R. M., de Lange, T., and Griffith, J. D. (2001) T-loop assembly in vitro involves binding of TRF2 near the 3′ telomeric overhang. *EMBO J.* *20*, 5532−5540.

(21) Sarek, G., Vannier, J. B., Panier, S., Petrini, J. H., and Boulton, S. J. (2015) TRF2 recruits RTEL1 to telomeres in S phase to promote t-loop unwinding. *Mol. Cell* *57*, 622−635.

(22) Ribes-Zamora, A., Indiviglio, S. M., Mihalek, I., Williams, C. L., and Bertuch, A. A. (2013) TRF2 interaction with Ku heterotetramerization interface gives insight into c-NHEJ prevention at human telomeres. *Cell Rep.* *5*, 194−206.

(23) Saint-Leger, A., Koelblen, M., Civitelli, L., Bah, A., Djerbi, N., Giraud-Panis, M. J., Londono-Vallejo, A., Ascenzioni, F., and Gilson, E. (2014) The basic N-terminal domain of TRF2 limits recombination endonuclease action at human telomeres. *Cell Cycle* *13*, 2469−2474.

(24) Biroccio, A., Rizzo, A., Elli, R., Koering, C. E., Belleville, A., Benassi, B., Leonetti, C., Stevens, M. F., D'Incalci, M., Zupi, G., and Gilson, E. (2006) TRF2 inhibition triggers apoptosis and reduces tumourigenicity of human melanoma cells. *Eur. J. Cancer* *42*, 1881−1888.

(25) Munoz, P., Blanco, R., Flores, J. M., and Blasco, M. A. (2005) XPF nuclease-dependent telomere loss and increased DNA damage in

mice overexpressing TRF2 result in premature aging and cancer. *Nat. Genet.* *37*, 1063−1071.
(26) Nakanishi, K., Kawai, T., Kumaki, F., Hiroi, S., Mukai, M., Ikeda, E., Koering, C. E., and Gilson, E. (2003) Expression of mRNAs for telomeric repeat binding factor (TRF)-1 and TRF2 in atypical adenomatous hyperplasia and adenocarcinoma of the lung. *Clin. Cancer Res.* *9*, 1105−1111.
(27) Brunori, M., Mathieu, N., Ricoul, M., Bauwens, S., Koering, C. E., Roborel de Climens, A., Belleville, A., Wang, Q., Puisieux, I., Decimo, D., Puisieux, A., Sabatier, L., and Gilson, E. (2006) TRF2 inhibition promotes anchorage-independent growth of telomerase-positive human fibroblasts. *Oncogene* *25*, 990−997.
(28) Cookson, J. C., and Laughton, C. A. (2009) The levels of telomere-binding proteins in human tumours and therapeutic implications. *Eur. J. Cancer* *45*, 536−550.
(29) Diehl, M. C., Idowu, M. O., Kimmelshue, K. N., York, T. P., Jackson-Cook, C. K., Turner, K. C., Holt, S. E., and Elmore, L. W. (2011) Elevated TRF2 in advanced breast cancers with short telomeres. *Breast Cancer Res. Treat.* *127*, 623−630.
(30) Simonet, T., Zaragosi, L. E., Philippe, C., Lebrigand, K., Schouteden, C., Augereau, A., Bauwens, S., Ye, J., Santagostino, M., Giulotto, E., Magdinier, F., Horard, B., Barbry, P., Waldmann, R., and Gilson, E. (2011) The human TTAGGG repeat factors 1 and 2 bind to a subset of interstitial telomeric sequences and satellite repeats. *Cell Res.* *21*, 1028−1038.
(31) Yang, D., Xiong, Y., Kim, H., He, Q., Li, Y., Chen, R., and Songyang, Z. (2011) Human telomeric proteins occupy selective interstitial sites. *Cell Res.* *21*, 1013−1027.
(32) El Mai, M., Wagner, K. D., Michiels, J. F., Ambrosetti, D., Borderie, A., Destree, S., Renault, V., Djerbi, N., Giraud-Panis, M. J., Gilson, E., and Wagner, N. (2014) The Telomeric Protein TRF2 Regulates Angiogenesis by Binding and Activating the PDGFRbeta Promoter. *Cell Rep.* *9*, 1047−1060.
(33) Biroccio, A., Cherfils-Vicini, J., Augereau, A., Pinte, S., Bauwens, S., Ye, J., Simonet, T., Horard, B., Jamet, K., Cervera, L., Mendez-Bermudez, A., Poncet, D., Gratarolí, R., de Rodenbeeke, C. T., Salvati, E., Rizzo, A., Zizza, P., Ricoul, M., Cognet, C., Kuilman, T., Duret, H., Lepinasse, F., Marvel, J., Verhoeyen, E., Cosset, F. L., Peeper, D., Smyth, M. J., Londono-Vallejo, A., Sabatier, L., Picco, V., Pages, G., Scoazec, J. Y., Stoppacciaro, A., Leonetti, C., Vivier, E., and Gilson, E. (2013) TRF2 inhibits a cell-extrinsic pathway through which natural killer cells eliminate cancer cells. *Nat. Cell Biol.* *15*, 818−828.
(34) Ovando-Roche, P., Yu, J. S., Testori, S., Ho, C., and Cui, W. (2014) TRF2-mediated stabilization of hREST4 is critical for the differentiation and maintenance of neural progenitors. *Stem Cells* *32*, 2111−2122.
(35) Burge, S., Parkinson, G. N., Hazel, P., Todd, A. K., and Neidle, S. (2006) Quadruplex DNA: sequence, topology and structure. *Nucleic Acids Res.* *34*, 5402−5415.
(36) Monchaud, D., and Teulade-Fichou, M. P. (2008) A hitchhiker's guide to G-quadruplex ligands. *Org. Biomol. Chem.* *6*, 627−636.
(37) Neidle, S. (2009) The structures of quadruplex nucleic acids and their drug complexes. *Curr. Opin. Struct. Biol.* *19*, 239−250.
(38) Tahara, H., Shin-Ya, K., Seimiya, H., Yamada, H., Tsuruo, T., and Ide, T. (2006) G-Quadruplex stabilization by telomestatin induces TRF2 protein dissociation from telomeres and anaphase bridge formation accompanied by loss of the 3′ telomeric overhang in cancer cells. *Oncogene* *25*, 1955−1966.
(39) Gomez, D., Wenner, T., Brassart, B., Douarre, C., O'Donohue, M. F., El Khoury, V., Shin-Ya, K., Morjani, H., Trentesaux, C., and Riou, J. F. (2006) Telomestatin induced telomere uncapping is modulated by POT1 through G-overhang extension in HT1080 human tumor cells. *J. Biol. Chem.* *281*, 38721−38729.
(40) Zhou, W. J., Deng, R., Zhang, X. Y., Feng, G. K., Gu, L. Q., and Zhu, X. F. (2009) G-quadruplex ligand SYUIQ-5 induces autophagy by telomere damage and TRF2 delocalization in cancer cells. *Mol. Cancer Ther.* *8*, 3203−3213.
(41) Pennarun, G., Granotier, C., Gauthier, L. R., Gomez, D., Hoffschir, F., Mandine, E., Riou, J. F., Mergny, J. L., Mailliet, P., and Boussin, F. D. (2005) Apoptosis related to telomere instability and cell cycle alterations in human glioma cells treated by new highly selective G-quadruplex ligands. *Oncogene* *24*, 2917−2928.
(42) Brassart, B., Gomez, D., De Cian, A., Paterski, R., Montagnac, A., Qui, K. H., Temime-Smaali, N., Trentesaux, C., Mergny, J. L., Gueritte, F., and Riou, J. F. (2007) A new steroid derivative stabilizes g-quadruplexes and induces telomere uncapping in human tumor cells. *Mol. Pharmacol.* *72*, 631−640.
(43) Gomez, D., Paterski, R., Lemarteleur, T., Shin-Ya, K., Mergny, J. L., and Riou, J. F. (2004) Interaction of telomestatin with the telomeric single-strand overhang. *J. Biol. Chem.* *279*, 41487−41494.
(44) Müller, S., and Rodriguez, R. (2014) G-quadruplex interacting small molecules and drugs: from bench toward bedside. *Expert Rev. Clin. Pharmacol.* *7*, 663−679.
(45) Murat, P., and Balasubramanian, S. (2014) Existence and consequences of G-quadruplex structures in DNA. *Curr. Opin. Genet. Dev.* *25*, 22−29.
(46) De Cian, A., Lacroix, L., Douarre, C., Temime-Smaali, N., Trentesaux, C., Riou, J. F., and Mergny, J. L. (2008) Targeting telomeres and telomerase. *Biochimie* *90*, 131−155.
(47) Rizzo, A., Salvati, E., Porru, M., D'Angelo, C., Stevens, M. F., D'Incalci, M., Leonetti, C., Gilson, E., Zupi, G., and Biroccio, A. (2009) Stabilization of quadruplex DNA perturbs telomere replication leading to the activation of an ATR-dependent ATM signaling pathway. *Nucleic Acids Res.* *37*, 5353−5364.
(48) Rodriguez, R., Miller, K. M., Forment, J. V., Bradshaw, C. R., Nikan, M., Britton, S., Oelschlaegel, T., Xhemalce, B., Balasubramanian, S., and Jackson, S. P. (2012) Small-molecule-induced DNA damage identifies alternative DNA structures in human genes. *Nat. Chem. Biol.* *8*, 301−310.
(49) Gray, L. T., Vallur, A. C., Eddy, J., and Maizels, N. (2014) G quadruplexes are genomewide targets of transcriptional helicases XPB and XPD. *Nat. Chem. Biol.* *10*, 313−318.
(50) Postberg, J., Tsytlonok, M., Sparvoli, D., Rhodes, D., and Lipps, H. J. (2012) A telomerase-associated RecQ protein-like helicase resolves telomeric G-quadruplex structures during replication. *Gene* *497*, 147−154.
(51) Paeschke, K., McDonald, K. R., and Zakian, V. A. (2010) Telomeres: structures in need of unwinding. *FEBS Lett.* *584*, 3760−3772.
(52) Gauthier, L. R., Granotier, C., Hoffschir, F., Etienne, O., Ayouaz, A., Desmaze, C., Mailliet, P., Biard, D. S., and Boussin, F. D. (2012) Rad51 and DNA-PKcs are involved in the generation of specific telomere aberrations induced by the quadruplex ligand 360A that impair mitotic cell progression and lead to cell death. *Cell. Mol. Life Sci.* *69*, 629−640.
(53) Redon, S., Bombard, S., Elizondo-Riojas, M. A., and Chottard, J. C. (2003) Platinum cross-linking of adenines and guanines on the quadruplex structures of the AG3(T2AG3)3 and (T2AG3)4 human telomere sequences in Na+ and K+ solutions. *Nucleic Acids Res.* *31*, 1605−1613.
(54) Ourliac-Garnier, I., Elizondo-Riojas, M. A., Redon, S., Farrell, N. P., and Bombard, S. (2005) Cross-links of quadruplex structures from human telomeric DNA by dinuclear platinum complexes show the flexibility of both structures. *Biochemistry* *44*, 10620−10634.
(55) Bertrand, H., Bombard, S., Monchaud, D., and Teulade-Fichou, M. P. (2007) A Platinum-Quinacridine Hybrid as G-Quadruplex Ligand. *JBIC, J. Biol. Inorg. Chem.* *12*, 1003−1014.
(56) Bertrand, H., Bombard, S., Monchaud, D., Talbot, E., Guedin, A., Mergny, J. L., Grunert, R., Bednarski, P. J., and Teulade-Fichou, M. P. (2009) Exclusive platination of loop adenines in the human telomeric G-quadruplex. *Org. Biomol. Chem.* *7*, 2864−2871.
(57) Gabano, E., Gama, S., Mendes, F., Gariboldi, M. B., Monti, E., Bombard, S., Bianco, S., and Ravera, M. (2013) Study of the synthesis, antiproliferative properties, and interaction with DNA and poly-nucleotides of cisplatin-like Pt(II) complexes containing carcinogenic polyaromatic amines. *JBIC, J. Biol. Inorg. Chem.* *18*, 791−801.
(58) Betzer, J. F., Nuter, F., Chtchigrovsky, M., Hamon, F., Kellermann, G., Ali, S., Calmejane, M.-A., Roque, S., Poupon, J.,

Cresteil, T., Teulade-Fichou, M. P., Marinetti, A., and Bombard, S. (2016) Linking of antitumour trans NHC-Pt(II) complexes to G-quadruplex DNA ligand for telomeric targeting. *Bioconjugate Chem.* *27*, 1456.
(59) Jung, Y., and Lippard, S. J. (2007) Direct cellular responses to platinum-induced DNA damage. *Chem. Rev.* *107*, 1387−1407.
(60) Ourliac Garnier, I., and Bombard, S. (2007) GG sequence of DNA and the human telomeric sequence react with cis-diammine-diaquaplatinum at comparable rates. *J. Inorg. Biochem.* *101*, 514−524.
(61) Jamieson, E. R., and Lippard, S. J. (1999) Structure, Recognition, and processing of Cisplatin-DNA Adducts. *Chem. Rev.* *99*, 2467−2498.
(62) Ishibashi, T., and Lippard, S. J. (1998) Telomere loss in cells treated with cisplatin. *Proc. Natl. Acad. Sci. U. S. A.* *95*, 4219−4223.
(63) Zhang, R. G., Zhang, R. P., Wang, X. W., and Xie, H. (2002) Effects of cisplatin on telomerase activity and telomere length in BEL-7404 human hepatoma cells. *Cell Res.* *12*, 55−62.
(64) Jeyapalan, J. C., Saretzki, G., Leake, A., Tilby, M. J., and von Zglinicki, T. (2006) Tumour-cell apoptosis after cisplatin treatment is not telomere dependent. *Int. J. Cancer* *118*, 2727−2734.
(65) Liu, M., Hales, B. F., and Robaire, B. (2014) Effects of four chemotherapeutic agents, bleomycin, etoposide, cisplatin, and cyclophosphamide, on DNA damage and telomeres in a mouse spermatogonial cell line. *Biol. Reprod.* *90*, 72.
(66) Ourliac-Garnier, I., Charif, R., and Bombard, S. (2009) Telomeres-Targets for Platinum Anticancer Drugs, in *Metal Complexes-DNA Interactions* (Hadjiliadis, N., and Sletten, E., Eds.) pp 209−234, Wiley-Blackwell.
(67) Burstyn, J. N., Heiger-Bernays, W. J., Cohen, S. M., and Lippard, S. J. (2000) Formation of cis-diamminedichloroplatinum(II) 1,2-intrastrand cross-links on DNA is flanking-sequence independent. *Nucleic Acids Res.* *28*, 4237−4243.
(68) Murray, V., and Kandasamy, N. (2012) The sequence specificity of the anti-tumour drug, cisplatin, in telomeric DNA sequences compared with consecutive guanine DNA sequences. *Anti-Cancer Agents Med. Chem.* *12*, 177−181.
(69) Ourliac-Garnier, I., Poulet, A., Charif, R., Amiard, S., Magdinier, F., Rezaï, K., Gilson, E., Giraud-Panis, M., and Bombard, S. (2010) Platination of telomeric DNA by cisplatin disrupts recognition by TRF2 and TRF1. *JBIC, J. Biol. Inorg. Chem.* *15*, 641−654.
(70) Gasnereau, I., Ganier, O., Bourgain, F., de Gramont, A., Gendron, M. C., and Sobczak-Thepot, J. (2007) Flow cytometry to sort mammalian cells in cytokinesis. *Cytometry, Part A* *71*, 1−7.
(71) Amiard, S., Doudeau, M., Pinte, S., Poulet, A., Lenain, C., Faivre-Moskalenko, C., Angelov, D., Hug, N., Vindigni, A., Bouvet, P., Paoletti, J., Gilson, E., and Giraud-Panis, M. J. (2007) A topological mechanism for TRF2-enhanced strand invasion. *Nat. Struct. Mol. Biol.* *14*, 147−154.
(72) Chtchigrovsky, M., Eloy, L., Jullien, H., Saker, L., Segal-Bendirdjian, E., Poupon, J., Bombard, S., Cresteil, T., Retailleau, P., and Marinetti, A. (2013) Antitumor trans-N-heterocyclic carbene-amine-Pt(II) complexes: synthesis of dinuclear species and exploratory investigations of DNA binding and cytotoxicity mechanisms. *J. Med. Chem.* *56*, 2074−2086.
(73) Wang, D., and Lippard, S. J. (2005) Cellular processing of platinum anticancer drugs. *Nat. Rev. Drug Discovery* *4*, 307−320.
(74) Brabec, V., and Kasparkova, J. (2005) Modifications of DNA by platinum complexes. Relation to resistance of tumors to platinum antitumor drugs. *Drug Resist. Updates* *8*, 131−146.
(75) Rodriguez, R., Müller, S., Yeoman, J. A., Trentesaux, C., Riou, J. F., and Balasubramanian, S. (2008) A novel small molecule that alters shelterin integrity and triggers a DNA-damage response at telomeres. *J. Am. Chem. Soc.* *130*, 15758−15759.
(76) Salvati, E., Leonetti, C., Rizzo, A., Scarsella, M., Mottolese, M., Galati, R., Sperduti, I., Stevens, M. F., D'Incalci, M., Blasco, M., Chiorino, G., Bauwens, S., Horard, B., Gilson, E., Stoppacciaro, A., Zupi, G., and Biroccio, A. (2007) Telomere damage induced by the G-quadruplex ligand RHPS4 has an antitumor effect. *J. Clin. Invest.* *117*, 3236−3247.
(77) Gomez, D., Guedin, A., Mergny, J. L., Salles, B., Riou, J. F., Teulade-Fichou, M. P., and Calsou, P. (2010) A G-quadruplex structure within the 5′-UTR of TRF2 mRNA represses translation in human cells. *Nucleic Acids Res.* *38*, 7187.
(78) Sears, C. R., Cooney, S. A., Chin-Sinex, H., Mendonca, M. S., and Turchi, J. J. (2016) DNA damage response (DDR) pathway engagement in cisplatin radiosensitization of non-small cell lung cancer. *DNA Repair* *40*, 35−46.
(79) Pennarun, G., Granotier, C., Hoffschir, F., Mandine, E., Biard, D., Gauthier, L. R., and Boussin, F. D. (2008) Role of ATM in the telomere response to the G-quadruplex ligand 360A. *Nucleic Acids Res.* *36*, 1741−1754.
(80) Pennarun, G., Hoffschir, F., Revaud, D., Granotier, C., Gauthier, L. R., Mailliet, P., Biard, D. S., and Boussin, F. D. (2010) ATR contributes to telomere maintenance in human cells. *Nucleic Acids Res.* *38*, 2955−2963.
(81) Munoz, P., Blanco, R., and Blasco, M. A. (2006) Role of the TRF2 telomeric protein in cancer and ageing. *Cell Cycle* *5*, 718−721.
(82) Nijjar, T., Bassett, E., Garbe, J., Takenaka, Y., Stampfer, M. R., Gilley, D., and Yaswen, P. (2005) Accumulation and altered localization of telomere-associated protein TRF2 in immortally transformed and tumor-derived human breast cells. *Oncogene* *24*, 3369−3376.
(83) Oh, B. K., Kim, Y. J., Park, C., and Park, Y. N. (2005) Up-regulation of telomere-binding proteins, TRF1, TRF2, and TIN2 is related to telomere shortening during human multistep hepatocarcinogenesis. *Am. J. Pathol.* *166*, 73−80.
(84) Hsu, C. P., Ko, J. L., Shai, S. E., and Lee, L. W. (2007) Modulation of telomere shelterin by TRF1 [corrected] and TRF2 interacts with telomerase to maintain the telomere length in non-small cell lung cancer. *Lung Cancer* *58*, 310−316.
(85) Granotier, C., Pennarun, G., Riou, L., Hoffschir, F., Gauthier, L. R., De Cian, A., Gomez, D., Mandine, E., Riou, J. F., Mergny, J. L., Mailliet, P., Dutrillaux, B., and Boussin, F. D. (2005) Preferential binding of a G-quadruplex ligand to human chromosome ends. *Nucleic Acids Res.* *33*, 4182−4190.
(86) Paeschke, K., Capra, J. A., and Zakian, V. A. (2011) DNA replication through G-quadruplex motifs is promoted by the Saccharomyces cerevisiae Pif1 DNA helicase. *Cell* *145*, 678−691.
(87) Ribeyre, C., Lopes, J., Boule, J. B., Piazza, A., Guedin, A., Zakian, V. A., Mergny, J. L., and Nicolas, A. (2009) The yeast Pif1 helicase prevents genomic instability caused by G-quadruplex-forming CEB1 sequences in vivo. *PLoS Genet.* *5*, e1000475.
(88) Piazza, A., Boule, J. B., Lopes, J., Mingo, K., Largy, E., Teulade-Fichou, M. P., and Nicolas, A. (2010) Genetic instability triggered by G-quadruplex interacting Phen-DC compounds in Saccharomyces cerevisiae. *Nucleic Acids Res.* *38*, 4337−4348.
(89) Piazza, A., Adrian, M., Samazan, F., Heddi, B., Hamon, F., Serero, A., Lopes, J., Teulade-Fichou, M. P., Phan, A. T., and Nicolas, A. (2015) Short loop length and high thermal stability determine genomic instability induced by G-quadruplex-forming minisatellites. *EMBO J.* *34*, 1718−1734.
(90) Huppert, J. L., and Balasubramanian, S. (2007) G-quadruplexes in promoters throughout the human genome. *Nucleic Acids Res.* *35*, 406−413.
(91) Biffi, G., Tannahill, D., McCafferty, J., and Balasubramanian, S. (2013) Quantitative visualization of DNA G-quadruplex structures in human cells. *Nat. Chem.* *5*, 182−186.
(92) Henderson, A., Wu, Y., Huang, Y. C., Chavez, E. A., Platt, J., Johnson, F. B., Brosh, R. M., Jr., Sen, D., and Lansdorp, P. M. (2014) Detection of G-quadruplex DNA in mammalian cells. *Nucleic Acids Res.* *42*, 860−869.
(93) Hansel-Hertsch, R., Beraldi, D., Lensing, S. V., Marsico, G., Zyner, K., Parry, A., Di Antonio, M., Pike, J., Kimura, H., Narita, M., Tannahill, D., and Balasubramanian, S. (2016) G-quadruplex structures mark human regulatory chromatin. *Nat. Genet.* *48*, 1267−1272.

(94) Hanaoka, S., Nagadoi, A., and Nishimura, Y. (2005) Comparison between TRF2 and TRF1 of their telomeric DNA-bound structures and DNA-binding activities. *Protein Sci. 14*, 119−130.
(95) Sfeir, A., and de Lange, T. (2012) Removal of shelterin reveals the telomere end-protection problem. *Science 336*, 593−597.
(96) Pagano, B., Amato, J., Iaccarino, N., Cingolani, C., Zizza, P., Biroccio, A., Novellino, E., and Randazzo, A. (2015) Looking for efficient G-quadruplex ligands: evidence for selective stabilizing properties and telomere damage by drug-like molecules. *ChemMedChem 10*, 640−649.